Available online at www.sciencedirect.com
ScienceDirect
Journal of the European Ceramic Society 30 (2010) 2819–2826
www.elsevier.com/locate/jeurceramsoc

# Effect of particle size on the shaping of ceramics by slip casting

Carolina Tallon [a], Monika Limacher [a,b], George V. Franks [a,*]

[a] *Chemical and Biomolecular Engineering, University of Melbourne, 3010 VIC, Australia*
[b] *Department of Nonmetallic Inorganic Materials, ETH Zurich, Switzerland*

Available online 20 April 2010

**Abstract**

The effect of the nanometric-ranged particle size of the starting powder through a simple and well-established shaping method, slip casting, has been studied. Several alumina suspensions with the same viscosity (but different solid content suspensions) and different particle size (11, 44, 190 and 600 nm) were prepared and shaped into a dense body. The green and sintered densities ranged between 30–67% and 63–99% of the theoretical value, respectively. These values, together with the microstructure observations reveal the effect of the solid content of the suspensions and the characteristics of the ceramic powder, leading to the determination of an optimal particle size. Based on both processability (rheological behaviour) and microstructure (density and grain size) it has been determined that particles with sizes ranging 100–300 nm are the best for preparing concentrated suspensions with low viscosity and bodies with density close to the theoretical value when using conventional pressureless sintering densification.


*Keywords:* Alumina; Nanoparticle; Suspension; Rheology; Sintering

## 1. Introduction

The interest in ceramic nanoparticles and their processing into nanomaterials and nanocomposites has led to their extensive study through a wide range of techniques and approaches for a variety of different applications. Ceramic nanopowders are expected to produce promising materials in terms of strength, hardness and wear. These fine-grained dense ceramics rely on the selection of low sintering temperatures to prevent grain growth to fulfill the required properties and microstructure for a specific application. But it is also necessary for the starting point for sintering to be a high green density body made of particles with large specific surface area to drive the desired densification. The preparation of high green density bodies is based on the preparation of high volume fraction and well dispersed suspensions, with low viscosity values, so that the suspensions can be formed into various complex shaped components. Very small particles have the large specific surface area needed to drive good densification, but they do not pack well into a green body since they cause a high suspension viscosity. The lower green density bodies are typically difficult to sinter unless special densification methods are used.[1–3] If particles somewhat larger are used, the fine-grained microstructure is not achieved. So the next question needs to be answered: can nanoparticles really lead to these fine-grained microstructures, when conventional pressureless sintering is used, to produce complex shaped components?

The routes that allow achieving the desired properties and microstructures often necessitate the handling of the nanopowders through the difficult preparation of stable suspensions. The nature and characteristics of nanoparticles result in very high viscosity suspensions for solid contents often lower than 20 wt.%.[4–7] The high excluded volume around the particles originating from the electric double layer or polymer layer adsorbed onto the surface to prevent agglomeration due to van der Waals attractive forces is one potential cause for high viscosity. Another reason for the high viscosity of the nanoparticle suspensions in the increase in electrolyte concentration associated with the high surface area of high volume fraction nanoparticle suspensions.[8] Although some authors have described suspensions up to 50 vol.% with relative low viscosity,[9,10] the typical low solids content is not enough to obtain ceramic pieces with high green density that produces final fully dense sintered bodies.

However, as mentioned before, this is not the only drawback to achieve a fully densified material from nanoparticles. First of all, their tendency to form agglomerates several times bigger than the primary particle size results in pores and heterogeneities

* Corresponding author. Tel.: +61 3 8344 9020; fax: +61 3 8344 4153.
*E-mail address:* gvfranks@unimelb.edu.au (G.V. Franks).

0955-2219/$ – see front matter © 2010 Elsevier Ltd. All rights reserved.
doi:10.1016/j.jeurceramsoc.2010.03.019

during the sintering step.[2] In addition, nanoparticles usually have a great reactivity as a consequence of a starting transition phase or higher specific surface area, which produce different driving forces during the densification, as explained by Legros et al.[11]

The effect of particle size, solid loading and surface chemistry in ceramic suspensions has been deeply investigated by different authors, especially in the range of submicron-sized particles, pointing out a key particle size distribution,[12,13] the need for a good stabilization mechanism created by one of several different additives[14–17] and successful routes for processing them into dense materials.[18] But when nanoparticles are to be employed, the traditional "know-how" about suspensions cannot be just transferred and applied as in the case of micron to submicron-sized particles, since the number of parameters and interactions to control is high, depending on the shaping technique selected to process the powder. A vast number of work has been conducting on this topic during the past couple of decades,[4,8,9,19] but still, a systematic study is required for complete understanding of the mechanism appearing in ceramic nanoparticle suspensions.

One of these examples of "know-how" is the homogenization of the suspensions using milling[20,21] or sonication[22] to prepare stable slurries for the shaping of ceramic materials. In these processes some new surfaces can be created or activated due to the breaking down of the agglomerates and/or decreasing the particle size. Sato et al.[20] and Hotta et al.[21] have used soft-energy milling (wet-jet and ball milling) with alumina (570 nm) suspensions of different solid content. The increase of solid content led to higher packing density of the green samples. The wet-jet milling just pulverized the alumina powder, and there are not changes in the surfaces. However, if the milling produces high collision energy, as in the case of ball milling, the surface of alumina is activated, increasing the attractive forces that cause refloculation of the suspension. This effect leads to increasing viscosity and green density changes but lower grain size and density after sintering. The more activated surfaces have a stronger driving force for densification, so the growth of the grains is faster and poor densification could be the result. The processing conditions used for nano-sized particles have to be re-studied.

So, can nanoparticles really lead to these fine-grained microstructures? Yes, but it is necessary to find and develop a guide to compromise "processability" of the powder and "final microstructure" by choosing the optimum particle size. Krell et al.[23,24] have reported that a closest ratio of powder particle size and sintered grain size could lead to the most fine-grained microstructure, selecting starting powders with sizes of 100–200 nm.

Previous work[8] studied the electrokinetic behaviour of particles in suspension and its effect upon particle size as a way to control the interactions developed inside the suspensions. Based on that, the present work studies the effect of particle size on the preparation of dense bodies, focusing on the control of the viscosity of the suspensions using particle sizes from submicron down to nanometric-size. In the present study, we use the suspension viscosity as the control variable (viscosity is maintained constant rather than volume fraction of solids). We use this control variable since suspension viscosity is the key parameter in determining success of processability in terms of mould filling for example. In order to achieve this, a traditional shaping method like slip casting has been selected, as well as electrical double layer stabilization mechanism for the suspension. We consider conventional pressureless sintering in order to densify the green bodies.

Table 1
Characteristics of powders selected for the present study.

| | Nanoamor | NanoTek | AKP-50 | AKP-15 |
|---|---|---|---|---|
| Crystalline phase | γ | γ | α | α |
| Average particle size (nm) | 11 | 44 | 190 | 600 |
| BET surface area ($m^2/g$) | 300 | 34 | 10 | 4 |
| Density ($g/cm^3$) | 3.70 | 3.66 | 3.98 | 3.98 |

## 2. Experimental

Four different alumina powders were used for this study: Nanoamor (Nanostructured & Amorphous Materials, Inc., USA), NanoTek (Nanophase Technologies Corp., USA), AKP-15 and AKP-50 (Sumitomo Chemical Company Ltd., Japan), presenting increasing particle size, as summarized in Table 1. Fig. 1 shows SEM images of the different powders.

Suspensions were prepared in deionized water at different solid contents and sonicated for 10 min (AKP-15 and AKP-50) and 30 min (Nanoamor and NanoTek) to break down agglomerates and homogenization. Electrical double layer repulsion was used as the stabilization mechanism for achieving proper dispersion. The pH was adjusted at 4.5 using $HNO_3$ to create positive charge on the alumina particles surfaces. The preparation of the suspensions is based in the previous work of Jailani et al.[8] The samples were rolled overnight to reach equilibrium. Solid content of each suspension was adjusted in order to achieve similar rheological behaviour for each type of particles (Table 2), i.e., producing low and high viscosity suspensions (referred to as LV and HV, respectively). Suspensions were slip cast into cylindrical PVC rings (20 mm diameter) placed over porous plaster. The green bodies were unmolded after 24 h of casting, then it took up to 5 days for total drying in air, and then placed at 105 °C in oven for at least 12 h. Samples were sintered at 1300–1500 °C for 2 h, with a heating rate of 5 °C/min up to 350 °C, with a dwell time of 30 min, 10 °C/min up to 1200 °C to try to overcome the $\gamma \rightarrow \alpha$ alumina phase transition before significant densification occurred, and 5 °C/min up to selected sintering temperature and further cooling down to room temperature.

Rheological behaviour was studied using a rheometer (RS5, Rheometric Scientific, USA) with a cone-plate configuration (diameter 40 mm, angle 0.0398 radians and gap 0.0483 mm). Suspensions were presheared for 30 s at 10 and 75 Pa for the low and high viscosity samples, respectively, and the viscosity curves were obtained by steady state shear viscosity measurement as the stress was increased over the range specified, from 0.1 to 20 Pa for low viscosity samples and 2 to 120 Pa for high viscosity ones. The green and sintered densities were determined by the Archimedes method in water, using wax to prevent water from penetrating pores in the case of green bodies. Densification

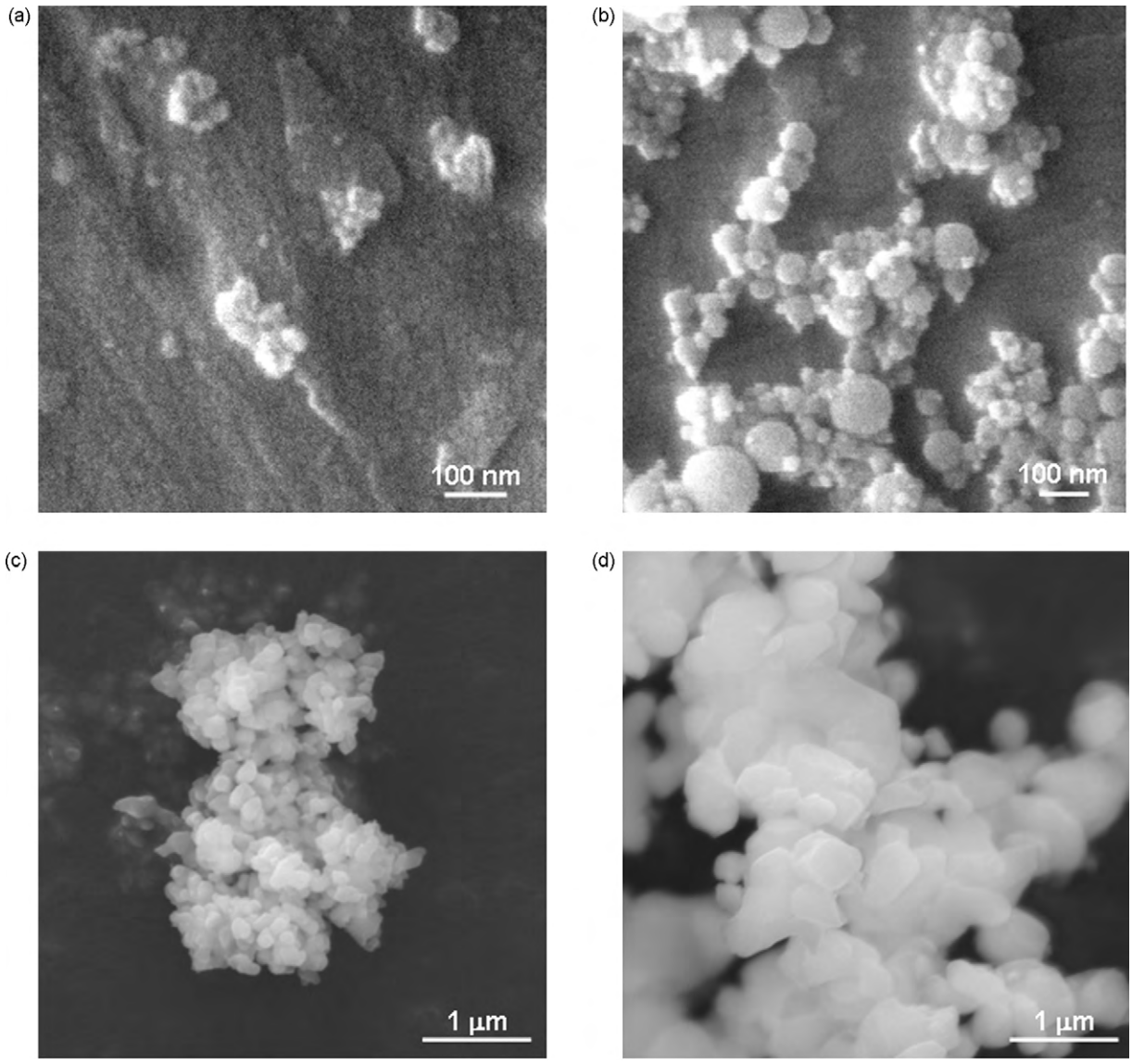


Fig. 1. SEM images of the starting material used in the present work: (a) Nanoamor 11 nm, (b) NanoTek 44 nm, (c) AKP-50 190 nm and (d) AKP-15 600 nm.

studies have been performed by registering dilatometric curves at 5 °C/min up to 1500 °C (402 E/7, Netszch, Germany) The microstructure of sintered specimens was observed by scanning electron microscopy, SEM (Philips XL-30) on polished and thermally etched surfaces at 1450 °C/10 min. The intercept length (∼2/3 of the grain size) was measured by line counting over several images for each sintering condition.

## 3. Results and Discussion

The results of the viscosity measurement for different suspensions of each type of particles are plotted in Fig. 2. The difference between low viscosity (LV) and high viscosity (HV) suspensions is approximately one order of magnitude. All of them show the same shear-thinning behaviour despite of different solid content selected in each case (Table 2), although the LV suspensions have a more Newtonian behaviour. The powders with smaller particle size and higher specific surface area, required lower solid content in suspension to obtain the same viscosity. This is related to the fact that the high specific surface area contributes to increase electrolyte concentration due to the dissociation of ionizable sites and soluble species and reduces the zeta potential and stability of suspensions, as explained elsewhere.[8] It is interesting to mention that the preparation of stable suspensions only by changing pH, i.e., electrical double layer stabilization mechanism, even for smaller particle size, has led to values close to those reported in the literature (20 vol.%) when dispersant is added for electrosteric stabilization.[25]

As it was mentioned before, the limited solid content for low viscosity nanoparticle suspensions is either related to the excluded volume around each particle or the higher salt content.[8] Both of these factors result in the fact that the smaller the particle size, the higher the viscosity of the suspension. Studart et al.[9] found a strong yielding behaviour, indicating that the nanoparticles agglomerate in a weakly attractive colloidal network that spans the entire suspension. Apparent viscosity values measured

Table 2
Solid content of suspensions and green densities values obtained for each condition.

| | | 11 nm | 44 nm | 190 nm | 600 nm |
|---|---|---|---|---|---|
| Solid content (vol.%) | Low viscosity | 12.5 | 25.5 | 34 | 52 |
| | High viscosity | 13.3 | 30.5 | 43 | 58 |
| Green density (g/cm$^3$) (%TD) | Low viscosity | 1.08 (29.2%) | 2.19 (60.0%) | 2.54 (63.9%) | 2.69 (67.5%) |
| | High viscosity | 1.01 (27.2%) | 2.18 (59.6%) | 2.49 (62.6%) | 2.62 (65.9%) |

by these researchers are similar to the ones presented in this work.

In typical ceramic casting slips using micron-sized particles, the average viscosity increases as particle size decreases, because the number of bonds between particles per unit of volume increases.[26] For average particles sizes less than 1 μm or for particles size distributions containing a significant fraction finer than 1 μm, pseudoplasticity is observed,[13] being in good agreement with the rheological behaviour observed for the suspensions described in the present work.

The relationship between particle size distribution and viscosity and packing in ceramic suspensions has been studied by different authors. Smith et al.[13] demonstrated that controlling the size distribution for particles finer than 15 μm provided the most desirable viscosity for slips composed of wide size distributions. Franks and Jailani[26] and Leong et al.[27] demonstrated that the rheological behaviour of nanoparticles suspensions depends inversely on the second power of primary particle size.

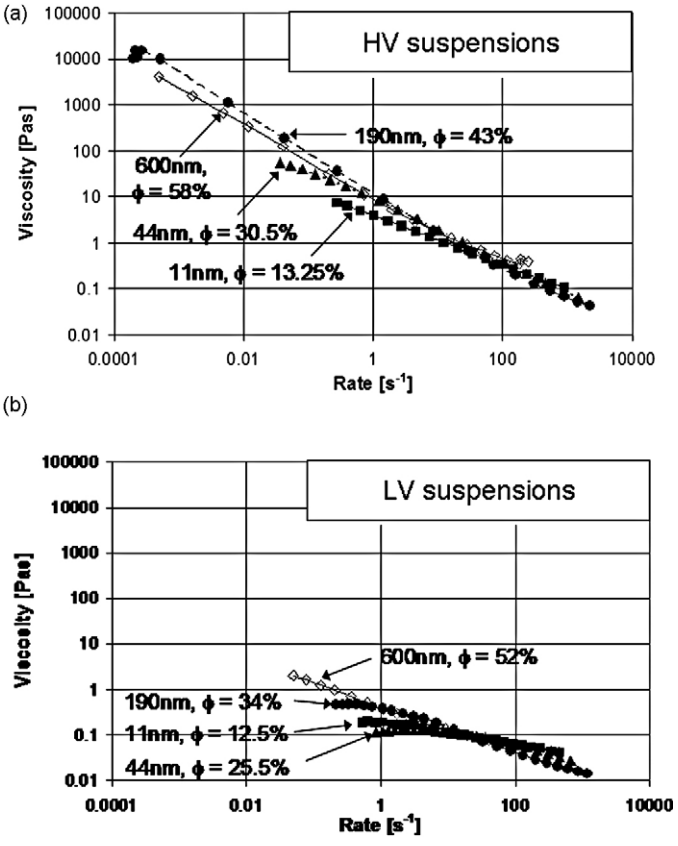


Fig. 2. Viscosity curves corresponding to the different suspensions prepared in (a) high viscosity and (b) low viscosity formulation, respectively.

The consolidation of the green bodies took place by the capillary suction of the plaster of Paris, drawing the water out of the suspension. Because of this reason, it is likely that some cracks appear in the green bodies (although too small to see by naked eye) when low viscosity suspensions for the smallest particles are used, resulting in green density value lower than 30% of the theoretical value for the 11 nm particles, as summarized in Table 2; however, the rest of the green density values were always above 60% of the theoretical value, increasing with particle size. It is worthy to note that the green densities for the lower particles sizes are around values usually associated to larger particle sizes. Bowen et al.[28] reported values of 34–50% TD for colloidal processing of transition aluminas (50 and 400 nm approximately) showing that the effect of pH in the conformation of the dispersant on the surface has an effect on the green packing density of the materials. The green density values measured for bodies prepared from LV suspensions were higher than those for the HV ones, suggesting that better dispersion produces better packing, easier consolidation and higher density bodies.

The connection between low viscosity suspensions and high green density bodies is well-known and extensively reported in literature for different systems, sizes and shaping methods, for a given solid content. For example, Sun et al.[29] prepared 70 wt.% suspensions with ZnO (260 nm) and $Al_2O_3$ (320 nm) for different dispersant percentage. After slip casting the slurries, the green density was higher (67% of theoretical value) for the suspension that reached the lower viscosity value (0.2% of PAA). Lindqvist et al.[30] prepared alumina suspensions of 50 vol.% with different latex content as a binder for solid freeform fabrication, reaching values of 63–64%TD for additions of latex of 0–1 wt.% that produces viscosities around 0.1 Pa s at 800 $s^{-1}$.

But the solid content of the suspension plays a determinant role in the green densities of materials. Huisman et al.[22] showed that the highest green density bodies are related to the higher solid content in suspension, reaching 68%TD for alumina (460 nm) suspensions of 57 vol.%, as a consequence of a closest particle coordination obtained by the self-arrangement of the particles due to the interparticle forces.[23] Ferreira and Diz[31] studied the effect of solid content of suspension with bimodal distribution of SiC particles upon green bodies prepared by slip casting. They found that at lower solid content, the particles have "more freedom" to rearrange during the deposition stage, promoting segregation phenomena and preventing an homogeneous packing; however, if the solid content increases, the deposition rate is higher and, together with the multiple interference between particles, there is a reduction of the segregation trend. If the solid content is further augmented, the particle rearrangement is hindered, resulting in lower packing.

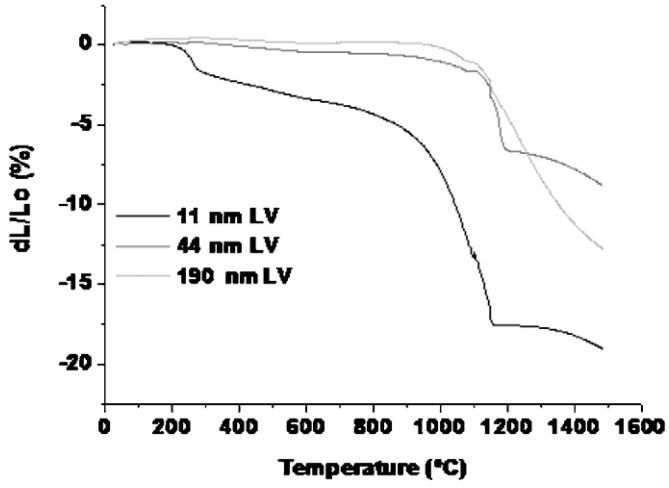


Fig. 3. Dilatometric curve at 5 °C/min up to 1550 °C for samples prepared from LV formulations for sizes 11, 44 and 190 nm.

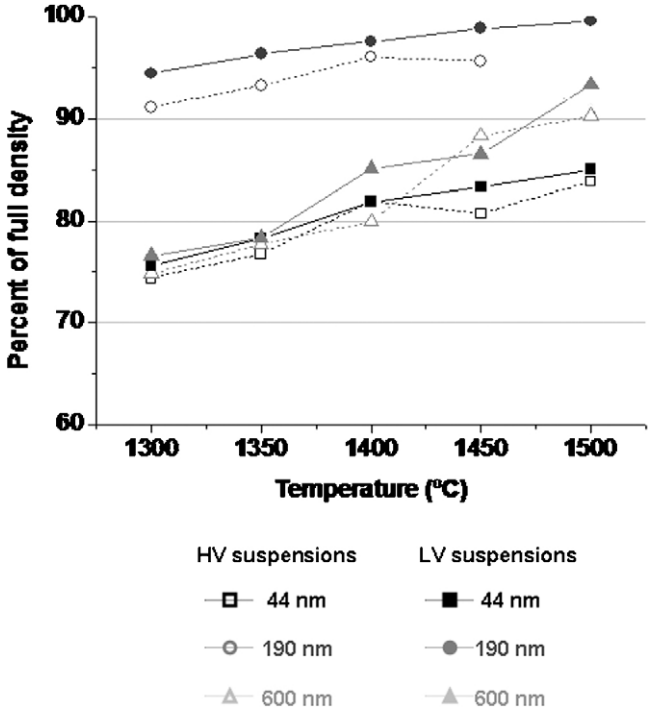


Fig. 4. Sintered density values versus temperature for samples prepared in the different conditions described.

In our case, the higher value of green density when LV formulations are used versus HV suspensions could be explained by the mobility and arrangement of particles during the casting. The suspensions have been formulated in a manner that it could be assume that the particle size distribution is narrow, with values closed to the primary particle size.[8] When the solid content is lower, the particles are "free" enough to move inside the suspension to achieve the lowest-free-energy dense packing. Since the suspension could be considered as a "monomodal" particle size distribution, there is no segregation, but a rearrangement towards maximum packing of the particles in the deposited cake-suspension interface, in comparison with the HV suspensions, where the rearrangement during consolidation is more hindered.

The influence of particle packing in green ceramics on the densification behaviour can be seen in the dilatometric curves plotted in Fig. 3. The higher shrinkage (20%) corresponds to the 11 nm sample, as expected, due to the lower solid content of the suspension employed for this material. The first shoulder observed correspond to the removal of water. The beginning of the sintering process involves the formation of sintering necks between particles, without changing the present porosity and without grain growth, related with the highest contraction.[11] The change of slope around 1100 °C represents the phase transformation from γ to α-$Al_2O_3$ involving the higher shrinkage rate, responsible of the shattering of the sample. A similar behaviour can be also noticed for the 44 nm sample, but the phase transformation takes place at temperature slightly higher due to the lower specific surface area, and therefore, less reactivity. The total shrinkage is lower than in the case of the 11 nm, as a consequence of the higher solid content and particle packing. However, the 190 nm sample does not show any remarkable change of slope, but a continuous shrinkage (up to 12%) associated to the densification of the material. For 44 and 190 nm it can be seen that the total contraction is lower, due to the increase of grain size and the closing of the remaining porosity.

The results of sintered densities as a function of sintered temperature and particle size are shown in Fig. 4. Samples corresponding to particle size of 11 nm shattered during firing due to the large amount of shrinkage. For the rest of the samples, the sintered density values were in the range 75–99% of the theoretical density of alumina (TD). The samples of 44 nm particles did not densify further than 85%TD due to the shrinkage associated with the relatively lower value of green density (60%) and to the phase transition from γ to α phase during sintering. The higher surface area of small particles results in greater driving force for densification, as it can be seen for the sample prepared with the particles of 190 nm in comparison to the 600 nm ones. Corresponding to the green density results, the highest final density values were reached for the LV suspensions, up to 99.5%TD for 190 nm particles sintered at 1500 °C.

The effect of the dispersion on green and sintered microstructures of slip cast bodies was explained by McAfee and Nettleship.[32] Their work studied the effect of two suspensions, flocculated and dispersed, with 20 vol.% solids content through different stages of sintering by means of pore boundary tessellation. This study revealed that the main differences in densification are related to the agglomerate structure present in the samples. Particles do not pack as efficiently when cast from flocculated slips, and the resultant low green density often increases the sintering time required to reach high density. Two different arguments have been proposed to explain this observation. One of them suggests that low green density results in enhanced grain growth during intermediate-stage densification and therefore a lower densification rate, while the second one is based on the argument that pores larger than a critical pore size to particle ratio will not shrink and be totally eliminated during sintering.[2,32–34]

The microstructure of sintered materials at 1400 °C for different particle size produced from LV suspensions is shown

Table 3
Grain size (intercept length) of sintered materials prepared through different sintering conditions from low viscosity slurries.

| $T_{sintering}$ (°C) | Intercept length (μm) | | |
|---|---|---|---|
| | 44 nm | 190 nm | 600 nm |
| 1300 | – | 0.84 | – |
| 1400 | 0.65 | 1.13 | 0.51 |
| 1500 | 1.06 | 1.74 | 1.11 |

in Fig. 5. The material prepared from 44 nm particles and LV suspensions reveals a heterogeneous microstructure; which has not reached full densification (82%TD). The grain size grew up to about a micron (intercept length 650 nm) as a consequence of the reactive surface of these particles (Table 3). In addition, materials obtained from 600 nm particles and LV suspensions did not totally densify either (85%), and the grain size observed is in the same range as the primary particles. In this case, surface is not reactive enough to drive mass transport and reach full densification. However, 190 nm particles in LV suspensions led to a densified microstructure with grain size around 1 μm and 97.5% of the theoretical density. Bowen et al.[2] suggested that for achieving full densities with final grain sizes <100 nm without grain growth in the final stage of densification, the relative kinetics of grain boundary movement and grain growth have to be controlled and tuned by means of two-step isothermal method or the use of vacuum sintering atmospheres, for example. Another method to retain fine grain size is the dual sintering and combined microwave with conventional heating.[1]

According to some authors,[21,29,30] the effect of viscosity and green density is not so strong on the sintering behaviour, being the temperature of sintering the major role for developing materials with density values close to the theoretical one, so different temperature for sintering were considered in this work. The microstructures of bodies corresponding to 190 nm particles and LV suspensions treated at different sintering temperatures are shown in Fig. 6. The grain size and density are higher with increasing temperature (Table 3), as expected, reaching values up to 99.5% TD after sintering at 1500 °C. In the case of 44 and 600 nm specimen treated at 1500 °C it can be observed that heterogeneities and porosity are still present, without reaching the fully dense microstructure desired. So, in the present work, the major effect on the sintering behaviour could be attributed to the viscosity and, in particular, the packing of the particles in the green body during the processing, and not to the temperature of sintering, since the green density difference between the HV and LV formulations is the threshold to achieve full densification.

Considering the rheological behaviour (for shape forming), particle packing in green body and final density and microstructure after sintering, there is an optimum particle size, 190 nm, that allows achieving the required conditions for an optimum shaping method, in terms of both processing and high density and fine grain microstructure, when conventional pressureless sintering is used. These results confirm the previous results pre-

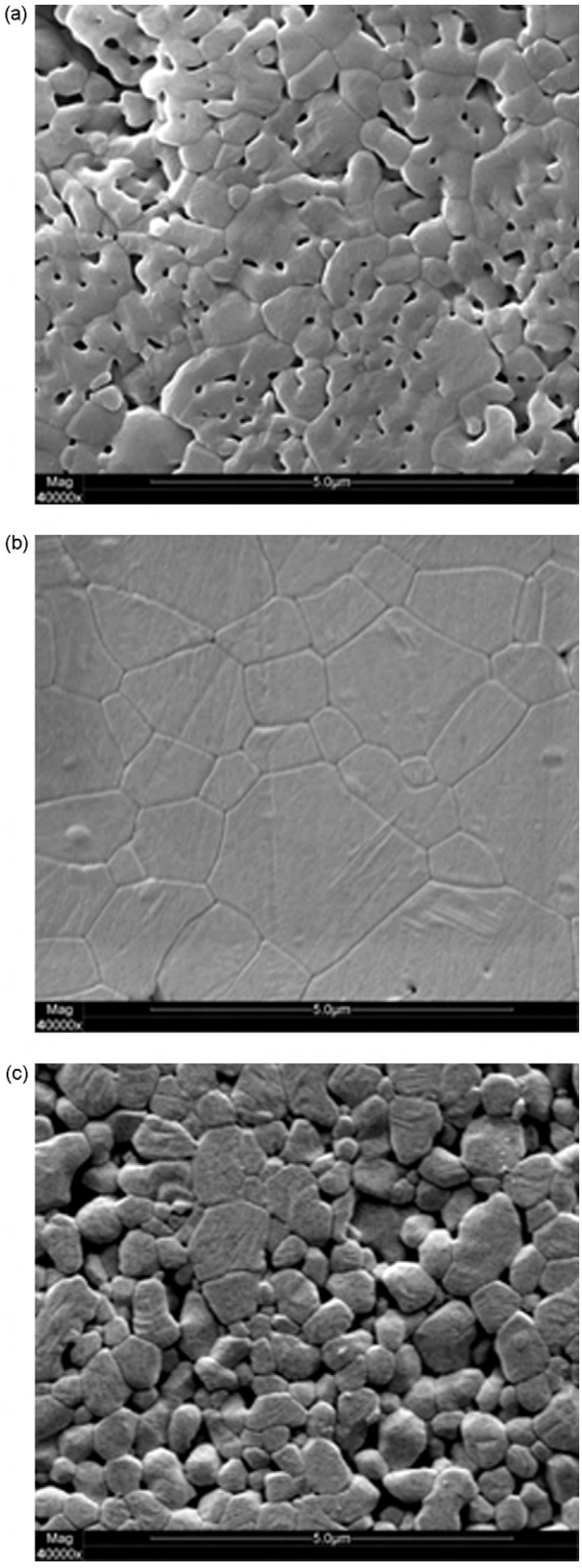


Fig. 5. SEM images corresponding to polished and thermally etched surfaces of sintered specimens at 1400 °C, prepared from the following formulations (a) 44 LV, (b) 190 LV and (c) 600 LV.

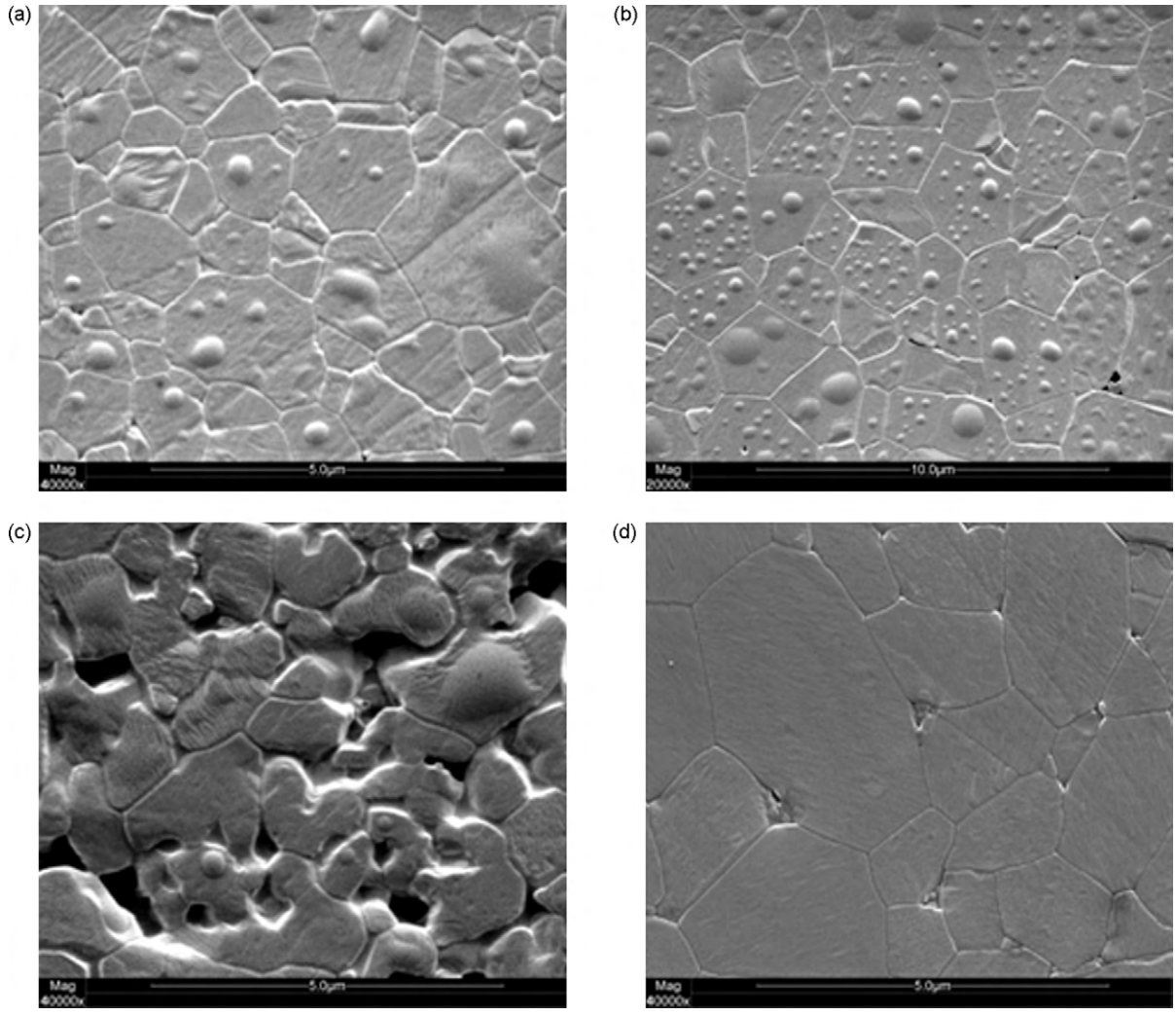


Fig. 6. SEM micrographs of polished and thermally etched surfaces of sintered specimens at different temperatures, corresponding to (a) 190 LV at 1300 °C, (b) 190 LV at 1500 °C, (c) 44 LV at 1500 °C and (d) 600 LV at 1500 °C.

sented by Krell et al.[23,24], where established a range close to 100–200 nm after a comparison between dry and wet processing routes at different sintering temperatures.

## 4. Conclusions

The effect of the particle size on the viscosity of suspensions for shaping of ceramic bodies has been studied. It has been observed that particles with sizes less than about 50–100 nm cannot produce low viscosity, high volume fraction suspensions (required to produce complex shapes by colloidal processing) and the resulting green density is too low to fully densify. In addition, particles larger than about 300–500 nm can produce low viscosity suspensions and high green density bodies, but in this case they do not have sufficient surface area to drive successful densification. However, it has been shown that particles with sizes ranging from 100 to 300 nm can be formulated as low viscosity, high volume fraction suspensions to produce green bodies of sufficiently high green density to fully densify (99% theoretical value), leading to homogeneous microstructures.

## Acknowledgements

The authors acknowledge support from the Australian Research Council (Discovery Project DP0879953). The authors also acknowledge Dr. Frank Filser and Prof. Ludwig Gauckler for sending Monika Limacher to the University of Melbourne, as well as extend the acknowledgement to Mrs. Socorro Benito (Instituto de Ceramica y Vidrio, CSIC (Madrid, Spain)) for the measurements of the dilatometric response of the materials. Thanks to Roger Curtain for SEM analysis and to Nigel Stone and Youseff Merchant for helping with the sintering of the samples.

## References

[1]. Binner J, Annapoorani K, Paul A, Santacruz I. Dense nanostructured zirconia by two stage conventional/hybrid microwave sintering. *J Eur Ceram Soc* 2008;**28**:973–7.

[2]. Bowen P, Carry C. From powders to sintered pieces: forming, transformation and sintering of nanostructured ceramic oxides. *Powder Technol* 2002;**128**:248–55.

[3]. Shen Z, Johnsson M, Zhao Z, Nygren M. Spark plasma sintering of alumina. *J Am Ceram Soc* 2002;**85**(8):1921–7.
[4]. Lu K, Kessler C. Colloidal dispersion and rheology study of nanoparticles. *J Mater Sci* 2006;**41**:5613–8.
[5]. Tseng WJ, Wu CH. Aggregation, rheology and electrophoretic packing structure of aqueous $Al_2O_3$ nanoparticles suspensions. *Acta Mater* 2002;**50**:3757–66.
[6]. Renger C, Kuschel P, Kristoffersson A, Clauss B, Oppermann W, Sigmund W. Rheology studies on highly filled nano-zirconia suspensions. *J Eur Ceram Soc* 2007;**27**:2361–7.
[7]. Tang F, Yu L, Huang X, Guo J. Characterization of adsorption and distribution of polyelectrolyte on stability of nano-zirconia suspensions by Auger electron microscopy. *Nanostruct Mater* 1999;**11**(4):441–50.
[8]. Jailani S, Franks GV, Healy TW. ζ potential of nanoparticle suspensions: effect of electrolyte concentration, particle size, and volume fraction. *J Am Ceram Soc* 2008;**91**(4):1141–7.
[9]. Studart AR, Amstad E, Antoni M, Gauckler LJ. Rheology of concentrated suspensions containing weakly attractive alumina nanoparticles. *J Am Ceram Soc* 2006;**89**(8):2418–25.
[10]. Xie Z, Ma J, Xu Q, Huang Y, Cheng Y-B. Effects of dispersants and soluble counter-ions on aqueous dispersability of nano-sized zirconia powder. *Ceram Int* 2000;**26**:93–7.
[11]. Legros C, Carry C, Bowen P, Hofmann H. Sintering of a transition alumna: effects of phase transformation, powder characteristics and thermal cycle. *J Eur Ceram Soc* 1999;**19**:1967–78.
[12]. Tari G, Ferreira JMF, Lyckfeldt O. Influence of the stabilizing mechanism and solid loading on slip casting of alumina. *J Eur Ceram Soc* 1998;**18**:479–86.
[13]. Smith PA, Haber RA. Reformulation of an aqueous alumina slip based on modification of particle-size distribution and particle packing. *J Am Ceram Soc* 1992;**75**(2):290–4.
[14]. Cesarano III J, I.A.Aksay IA. Processsing of highly concentrated aqueous α-alumina suspensions stabilized by polyelectrolytes. *J Am Ceram Soc* 1988;**71**(12):1062–7.
[15]. Cesarano III J, Aksay IA, Bleier A. Stability of aqueous α-alumina suspensions with poly(methacrylic acid) polyelectrolyte. *J Am Ceram Soc* 1988;**71**(4):250–5.
[16]. Hidber PC, Graule TJ, Gauckler LJ. Citric acid-a dispersant for aqueous alumina suspensions. *J Am Ceram Soc* 1996;**79**(7):1857–67.
[17]. Hidber PC, Graule TJ, Gauckler LJ. Influence of the dispersant structure on properties of electrostatically stabilized aqueous alumina suspensions. *J Eur Ceram Soc* 1997;**17**:239–49.
[18]. Sigmund WM, Bell NS, Bergström L. Novel powder-processing methods for advanced ceramics. *J Am Ceram Soc* 2000;**83**(7):1557–74.
[19]. Li C, Akinc M. Role of bound water on the viscosity of nanometric alumina suspensions. *J Am Ceram Soc* 2005;**88**(6):1448–54.
[20]. Sato K, Hotta Y, Yilmaz H, Watari K. Fabrication of green and sintered bodies prepared by centrifugal compaction process using wet-jet milled slurries. *J Eur Ceram Soc* 2009;**29**:1323–9.
[21]. Hotta Y, Tsunekawa K, Shirai T, Sato K, Yasokua M, Watari K. Fabrication of stable $Al_2O_3$ slurries and dense green bodies using soft-energy milling process. *J Eur Ceram Soc* 2009;**29**:869–74.
[22]. Huisman W, Graule T, Gauckler LJ. Alumina of high reliability by centrifugal casting. *J Eur Ceram Soc* 1995;**15**:811–21.
[23]. Krell A, Blank P, Ma H, Hutzler T, Nebelung M. Processing of high-density submicrometer $Al_2O_3$ for new applications. *J Am Ceram Soc* 2003;**86**(4):546–53.
[24]. Krell A, Klimke J, Hutzler T. Advanced spinel and sub-μm $Al_2O_3$ for transparent armour applications. *J Eur Ceram Soc* 2009;**29**:275–81.
[25]. Lu K, Kessler CS, Davis RM. Optimization of a nanoparticle suspension for freeze casting. *J Am Ceram Soc* 2006;**89**(8):2459–65.
[26]. Franks GV, Jailani S. Nano-particle suspension rheology: effect of particle size. In: *Proceedings of Chemeca 2007*. 2007.
[27]. Leong YK, Scales PJ, Healy TW, Boger DV. Effect of particle-size on colloidal zirconia rheology at the isoelectric point. *J Am Ceram Soc* 1995;**78**:2209–13.
[28]. Bowen P, Carry C, Luxembourg D, Hoffmann H. Colloidal processing and sintering of nanosized transition aluminas. *Powder Technol* 2005;**157**:100–7.
[29]. Sun Y-H, W.-H. Xiong W-H, Li C-H, Yang L. Effect of dispersant concentration on preparation of an ultrahigh density ZnO–$Al_2O_3$ target by slip casting. *J Am Ceram Soc* 2009;**92**(9):2168–71.
[30]. Lindqvist KM, Carlstrom E. Indirect solid freeform fabrication by binder assisted slip casting. *J Eur Ceram Soc* 2005;**25**:3539–45.
[31]. Ferreira JMF, Diz HMM. Effect of solid loadings on slip-casting performance of silicon carbide slurries. *J Am Ceram Soc* 1999;**82**(8):1993–2000.
[32]. McAfee RJ, Nettleship I. Effect of slip dispersion on microstructure evolution during isothermal sintering of cast alumina. *J Am Ceram Soc* 2006;**89**(4):1273–9.
[33]. Slamovich EB, Lange FF. Densification of large pores. I. Experiments. *J Am Ceram Soc* 1992;**75**(9):2498–508.
[34]. Slamovich EB, Lange FF. Densification of large pores. II. Driving potentials and kinetics. *J Am Ceram Soc* 1993;**76**(6):1584–90.